Canadian Mineralogist
Vol. 26, pp. 755-763 (1988)

THE NATURE AND ORIGIN OF SMECTITE IN THE ATLANTIS II DEEP, RED SEA

THOMAS G. COLE

*Department of Chemistry, Imperial College of Science and Technology, London, SW7 2AY, England**

ABSTRACT

Authigenic smectite dominates the silicate mineralogy of sediments underlying the hot brine pools of the Atlantis II Deep geothermal system in the Red Sea. Chemical compositions for monomineralic smectite fractions separated from three different facies give formulae that possibly distinguish three smectite species, one from each facies: (1) trioctahedral Mg-rich smectite (iron-bearing saponite) formed at high temperature (~160–200°C) under anoxic conditions in close proximity to intense brine venting (Sulfate/Sulfide/Silicate/Oxide facies, dominated by anhydrite); (2) dioctahedral Fe-rich smectite (nontronite) formed at lower temperature (~80°C) under oxic, more quiescent conditions in the periphery of the brine pool (Silicate/Carbonate/Oxide facies, including abundant detrital material and hydrated iron oxides); (3) intermediate dioctahedral/trioctahedral Fe-rich smectite formed at intermediate temperatures (~90–140°C) under anoxic conditions occupying the greater volume of the brine pool and sediments (Sulfide/Silicate/Amorphous facies, dominated by the smectite). The smectites may be members in a coherent solid-solution series of trioctahedral/dioctahedral Mg/Fe fractionation, spatially related to temperature and redox conditions. The saponite approaches the high-temperature trioctahedral Mg end-member, assumed to be talc. The oxic, low-temperature nontronite is almost the dioctahedral Fe end-member. The anoxic Fe-rich smectite is intermediate, having a mixed di-/trioctahedral structure, including significant Zn and Cu, and containing some Mg substitution.

Keywords: smectite, saponite, nontronite, mixed di-/trioctahedral smectite, Mg–Fe fractionation, geothermal system, Atlantis II Deep, Red Sea.

SOMMAIRE

La smectite authigène constitue le silicate le plus volumineux des sédiments sous les bassins de saumures chaudes des systèmes géothermiques situés dans l'abysse de Atlantis II, dans la mer Rouge. La composition chimique des fractions monominéraliques de smectite, isolées des trois facies différents, mène à des formules chimiques qui permettent la distinction de trois variantes de smectite, une dans chaque facies: 1) smectite trioctaédrique magnésienne (saponite ferrifère), cristallisée à température élevée (~160–200°C) à des conditions anoxyques, à forte proximité des évents de saumure (facies à sulfate–sulfure–silicate–oxyde, à forte teneur en anhydrite): 2) smectite dioctaédrique ferrifère (nontronite), cristallisée à température plus basse (~80°C) dans un milieu plus oxygéné et plus calme, à la périphérie des bassins de saumure (facies silicate–carbonate–oxyde, avec abondance de matériaux détritiques et d'oxydes de fer hydratés); 3) smectite intermédiaire, à caractère dioctaédrique – trioctaédrique, cristallisée à une température intermédiaire (~90–140°C) dans un milieu anoxyque, et typique de la portion la plus volumineuse des bassins ainsi que des sédiments sous-jacents (facies sulfure–silicate–oxydes amorphes, où la smectite est la phase dominante). Les trois variantes pourraient faire partie d'une solution solide cohérente en termes de fractionation de Mg et de Fe, et d'évolution du caractère trioctaédrique – dioctaédrique, dont la composition résulterait d'une zonation de la température et des conditions d'oxydoréduction dans l'espace. La saponite se rapproche du pôle trioctaédrique magnésien stable à température élevée, supposé être le talc. La nontronite de basse température, oxygénée, se rapproche du pôle dioctaédrique ferrifère. La smectite riche en fer et anoxyque est intermédiaire dans son caractère mixte di-/trioctaédrique, la présence de teneurs appréciables en Zn et en Cu, et la substitution de magnésium au fer.

(Traduit par la Rédaction)

Mots-clés: smectite, saponite, nontronite, smectite à caractère di-/trioctaédrique mixte, fractionation Mg–Fe, système géothermique, abysse de Atlantis II, mer Rouge.

INTRODUCTION

The geothermal brine system of the Atlantis II Deep (Red Sea) has been studied intensively during the last 20 years. Consequently, the nature and origin both of the hot brines that fill the Deep and the metalliferous sediments precipitating on its floor are well-documented (*e.g.*, Degens & Ross 1969, Bäcker & Richter 1973, Shanks & Bischoff 1977, Pottorf & Barnes 1983). Particular attention has been focused on the silicate assemblage of the sediments, predominantly iron-rich smectite (Bischoff 1972, Hackett & Bischoff 1973, Goulart 1976, Cole & Shaw 1983a, Zierenberg & Shanks 1983, Badaut *et al.* 1985).

This paper is a sequel to an oxygen isotope study of smectite in the Atlantis II Deep (Cole 1983). The primary objective is to report chemical compositions for the smectite samples. On this basis, previous conclusions concerning the nature and origin of the smectite are modified.

SAMPLE MATERIAL

Several major laterally correlative lithostratigraphic units or facies have been defined for the Atlantis

* Present address: Divisione Radiochimica (Ed. 46), CCR EURATOM, 21020, Ispra, (Varese), Italy.

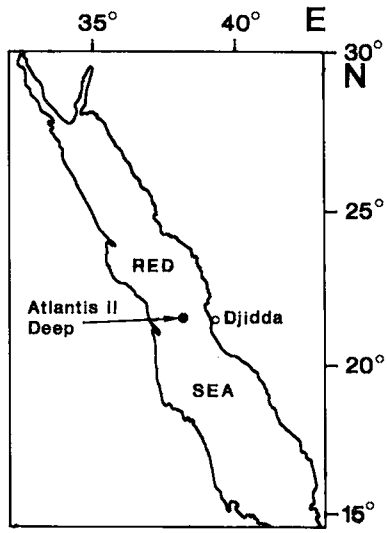

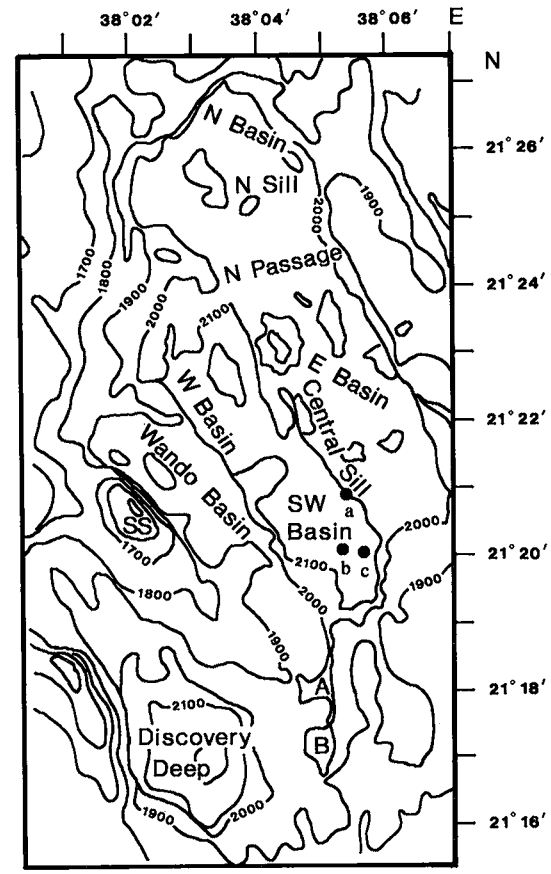

FIG. 1. Location (top) and physiography (right) of the Atlantis II Deep area. Contours in corrected meters (after Bäcker & Schoell 1972). The 2000-m contour outlines the presence of brine pools (accoustic top of salinity anomaly). A and B are Chain Deeps. SS is Signal Seamount; a, b, and c are positions of cores 10094, 10096, and 10097, respectively.

TABLE 1. FIRST BASAL REFLECTION SPACINGS, *d*, OF CLAY FRACTIONS (<2μm) FROM SILICATE-CONTAINING FACIES IN CORES 10094, 10096, AND 10097, AFTER DIAGNOSTIC TREATMENTS

Core Number	Sample Interval (cm)	Air Dried (Å)	Glycerated (Å)	400°C (Å)	600°C (Å)	Facies
10094	0 - 10	13	16.5	9.5	9	
	50 - 55	12.5	16.5	10	9.5	SSA
	105 - 110	13	15	10	9.5	
10094	253 - 258	13	17	9.5	9.5	SCO
	265 - 270	13	18	14.5	10	
10096	15 - 20	13	14.5	10	9.5	
	70 - 75	13	17	9.5	9	SSA
	100 - 105	12	16.5	9.5	9.5	
10097	0 - 10	12	14	9.5	9.5	SSA
	45 - 50	11.5	15.5	9.5	9.5	
10097	70 - 75	11.5	18	10	10	
	90 - 95	13	18	15	9.5	
	120 - 125	12	18	10	9	SSSO
	200 - 205	11.5	18	10	9.5	
	260 - 265	12	18	10	9.5	

TABLE 2. 02 AND 06 SPACINGS, *d*, OF SMECTITES IN CORES 10094, 10096, AND 10097

Core Number	Sample Interval (cm)	020 (Å)	060 (Å)	Facies
10094	5 - 10	4.61 - 4.51	-	
	18 - 25	?	-	
	58 - 62	?	-	
	105 - 110	?	-	
	121 - 129	4.53	-	SSA
10096	0 - 10	4.57	-	
10097	0 - 10	4.57	-	
	0 - 4	4.53	-	
10094	252 - 260	4.53	-	SCO
10097	179 - 184	4.57	1.53	
	207 - 212	4.57	1.53	SSSO
	247 - 252	4.59	1.53	

II Deep sediments (Bischoff 1969, Bäcker & Richter 1973, Hackett & Bischoff 1973). These reflect distinct episodes of depositional conditions related to periodic variations in the flux of the discharging brine (Shanks & Bischoff 1980). However, locally the active brine system supports a continually changing and wide range of temperatures and oxygen fugacities. Thus, fine-scale (dm to cm) interbedding of sulfides, sulfates, silicates, oxides, and carbonates is common, including intermixing of phases in a variety of combinations. Similar variety was evident in three cores (10094 and 10097, both 2.7 m long, and 10096, 1 m long) used for both this study and that of Cole (1983). All were recovered from the Southwest (SW) Basin of the Atlantis II Deep (Fig. 1), an area consi-

TABLE 3. BASAL SPACINGS, $d(001)$ (in Å), OF SSSO-FACIES SMECTITE, AFTER DIAGNOSTIC TREATMENTS (INCLUDING REFERENCE DATA FROM: SUQUET ET AL. 1975, MacEWAN & WILSON 1980, BROWN & BRINDLEY 1980)

Sat. cation	Na				Mg				Li (Greene-Kelly Test)	
Solv. complex	Air[4] Dried	Glycol	Glycerol	Water	Air[4] Dried	Glycol	Glycerol	Water	Overnight heat. 250 - 300°C	Glycerol Solvated
179 - 184 cm	12.5	-	18.0	-	-	-	-	-	-	-
200 - 205 cm	-	-	18.0	-	14.5	-	-	18.7	10.1	15.8
207 - 212 cm	12.5	-	18.0	-	14.6	16.6	17.7	-	-	-
247 - 252 cm	12.4 9.8	-	18.0	-	14.8 11.4	16.8	17.7	-	-	-
Montmorillonite	12.5	17	17.8	-	15	17	17.8	19.4	9.5	9.5
Beidellite[1]	-	16.9	18	-	-	17	18	18.6	9.5	17.7
Saponite (anhyd.)[2]	9.7									
Saponite (monohyd.)[2]	12.4	16.7	18.1	15.2	11.4	16.7	18.1	18.9	-	17.7
Saponite (dihyd.)[2]	15.3				14.6					
Vermiculite[3]	12.5	14.8	14.8	14.9	14.5	14.3	14.3	14.7	-	-

1. Displays variable hydration similar to saponite (Suquet et al. 1975).
2. anhyd. = no interlayer water; monohyd. = one water layer; dihyd. = two water layers.
3. Included for comparison.
4. Literature data for Air Dried spacings are approximate.

TABLE 4. CHEMISTRY OF ATLANTIS II DEEP SMECTITE[1]

Core Number	Sample Interval (cm)	SiO_2 %	Al_2O_3 %	Fe_2O_3 Total %	MgO %	CaO %	Na_2O %	K_2O %	MnO^3 %	TiO_2[4] %	Zn %	Cu %	Ni[3] %	H_2O %	Σ[5] %	Facies
10094	5 - 10	39.8	2.1	34.8	1.4	0.6	0.7	0.2	-	-	4.2	1.3	-	nd		SSA
10094 and[2]	18 - 25	36.8	2.0	32.0	1.4	0.6	4.2	0.2	-	-	3.2	0.9	-	17.5	99.4	SSA
	58 - 62	37.5	2.0	32.5	1.4	0.4	3.1	0.2	-	-	4.4	1.0	-			
10094 and[2]	105 - 110	36.0	1.7	28.9	1.6	0.7	2.4	0.6	-	-	2.7	0.5	-	nd		SSA
	121 - 129	36.3	1.7	29.3	1.6	0.6	2.4	0.6	-	-	3.2	1.1	-			
10096	0 - 10	40.4	2.2	29.2	1.3	0.5	2.6	0.3	-	-	3.7	0.6	-	18.7	99.5	SSA
10097	0 - 10	38.1	2.1	29.1	1.6	0.8	3.1	0.2	0.1	-	3.8	0.9	-	19.4	99.8	SSA
		38.6	2.2	29.4	1.6	0.8	3.2	0.2	0.1	-	3.6	0.8	-			
10094	252 - 260	46.4	0.3	32.9	0.4	0.1	3.9	0.1	-	-	0.4	0.3	-	16.2	101.4	SCO
		46.4	0.4	33.1	0.5	0.1	3.9	0.1	-	-	0.4	0.5	-			
10097	179 - 184	46.6	5.0	8.2	23.6	0.8	3.6	-	-	-	0.2	0.1	-	13.0	101.8	SSSO
		47.2	5.0	8.4	24.0	0.8	3.6	-	-	-	0.3	0.1	-			
10097	207 - 212	40.6	5.3	12.7	19.2	0.3	6.6	-	-	-	0.2	-	-	14.4 14.4	99.3	SSSO
10097	247 - 252	52.7	3.3	4.2	27.9	0.2	2.1	-	-	-	0.2	-	-	11.1 11.3	101.8	SSSO
HRM 1[6]		87.9	2.6	1.2	0.1	0.1	0.2	1.2	-	0.1	-	-	-			
		89.9	2.6	1.4	0.1	0.1	0.3	1.2	-	0.1	-	-	-			
Acc.		92.0	2.7	1.3	0.1	0.1	0.3	1.3	-	0.1	-	-	-			
HRM 2[6]		57.2	9.6	7.5	3.3	1.3	0.8	1.9	0.2	0.6	-	-	-			
		58.7	9.8	7.8	3.4	1.3	0.8	2.0	0.2	0.6	-	-	-			
Acc.		57.8	9.9	7.7	3.5	1.3	0.9	2.0	0.2	0.5	-	-	-			

1. - indicates <0.05%; nd indicates not determined.
2. Combined intervals due to sample shortage; justified by their chemical similarity.
3. Included to indicate absence of contaminant ferromanganese phases.
4. Included to indicate absence of contaminant detrital/volcanic phases.
5. Σ is the sum (average where duplicate data are given).
6. HRM 1 and HRM 2 are House Reference Materials (Acc. = Accepted Value).

dered to be the locus of present-day brine discharge (Schoell & Hartmann 1973). To clarify local depositional zones specific to the cores, their facies makeup has been redefined (Cole 1982, 1983) to include three silicate-containing combinations:

1) SSA (Sulfide/Silicate/Amorphous) facies (10094: 0–130 cm; 10096: 0–110 cm; 10097: 0–70 cm)

2) SCO (Silicate/Carbonate/Oxide) facies (10094: 250–270 cm)

3) SSSO (Sulfate/Sulfide/Silicate/Oxide) facies (10097: 70-270 cm)

Analytical Methods and Results

Reliable chemical and isotopic composition determinations of clay minerals require the separation of monomineralic samples. Preliminary XRD analysis of the clay fraction (<2 μm) separated from each silicate-containing facies (Tanner & Jackson 1947) was achieved with FeKα radiation (in vacuo, 1°/min) using oriented mounts (Shaw 1972) of material treated with bicarbonate-buffered citrate/dithionite (BCD) reagent (Mehra & Jackson 1960). Clay-mineral identification was assisted using routine diagnostic treatments, glycerol solvation and heating (Table 1). Isolation of pure smectite was accomplished by centrifugation to obtain the <0.5 μm fraction following BCD treatment of bulk sediment. Smectite typically concentrates in the finest fractions of sediments. The BCD treatment dissolves hydrated iron oxides and enhances sample dispersion. XRD analysis of the separates as smear mounts using Co-Kα radiation confirmed that they are monomineralic smectite. Further XRD analyses of the separates

TABLE 5. ATOMIC PROPORTIONS AND SITE OCCUPANCY PER UNIT CELL OF ATLANTIS II DEEP SMECTITES[1]

	Sample ID/Facies[2]								
Tet. layer ions[3]	SSA					SCO	SSSO		
	A	B	C	D	E	F	G	H	I
Si^{4+}	6.90	6.75	6.98	7.20	6.99	7.51	6.88	6.51	7.28
Al^{3+}	0.43	0.44	0.39	0.47	0.46	0.07	0.87	1.00	0.54
Fe^{3+}	0.67	0.81	0.63	0.33	0.55	0.42	0.25	0.49	0.18
Total	8.00	8.00	8.00	8.00	8.00	8.00	8.00	8.00	8.00
Oct. layer ions[4]									
Fe^{3+}	2.41	2.18	2.24	2.33	2.18	3.59	-	-	-
Fe^{2+}	1.45	1.41	1.35	1.25	1.28	-	0.67	1.04	0.26
Al^{3+}	-	-	-	-	-	-	-	-	-
Mg^{2+}	0.37	0.38	0.47	0.35	0.44	0.11	5.21	4.60	5.74
Zn^{2+}	0.67	0.64	0.52	0.61	0.62	0.06	0.04	0.02	0.03
Cu^{2+}	0.21	0.17	0.14	0.10	0.15	0.06	0.01	-	0.01
Total	5.11	4.78	4.72	4.64	4.67	3.82	5.93	5.66	6.04
Int. layer ions									
Na^{+}	0.23	1.29	0.90	0.90	1.12	1.22	1.03	2.06	0.56
K^{+}	0.04	0.04	0.16	0.07	0.05	0.02	-	-	0.01
Ca^{2+}	0.11	0.10	0.13	0.10	0.15	0.01	0.13	0.05	0.03
Total	0.38	1.43	1.19	1.07	1.32	1.25	1.16	2.11	0.60
Tet. excess charge	-1.10	-1.25	-1.02	-0.80	-1.01	-0.49	-1.12	-1.49	-0.72
Oct. excess charge	+0.63	-0.26	-0.32	-0.39	-0.48	-0.77	-0.14	-0.68	+0.08
Total excess charge	-0.47	-1.51	-1.34	-1.19	-1.49	-1.26	-1.26	-2.17	-0.64

1. Based on 20 oxygen atoms and 4 hydroxyl groups per formula unit.
2. A 10094, 5-10 cm; B 10094, 18-25 cm and 58-62 cm, combined; C 10094, 105-110 cm and 121-129 cm, combined; D 10096, 0-10 cm; E 10097, 0-10 cm; F 10094, 252-260 cm; G 10097, 179-184; H 10097, 207-212 cm; I 10097, 247-252 cm.
3. Fe^{3+} assigned to tetrahedral layer (compensating for an Al^{3+} deficiency in all samples) in exactly the desired amount to afford a full complement of 8 atoms per unit cell.
4. Refer to text for justification of bulk iron apportionment between Fe^{2+} and Fe^{3+} valency states in octahedral layer.
- indicates no assignment.

(SSSO facies in particular), including Mg^{2+} saturation, glycol *versus* glycerol solvation, use of CuKα radiation, and the Greene-Kelly test involving Li^{+} saturation (MacEwan & Wilson 1980) also were performed to assist species identification (Tables 2, 3).

The chemistry of the smectite separates was determined following $LiBO_2$ fusion (Ingamells 1970) by ICP emission spectroscopy (Table 4). Water contents of the samples were determined by weight loss on ignition at 950°C for 50 minutes, which removes both interlayer water and hydroxyl water. Based on the procedure of Ross & Hendricks (1945), the chemical compositions were used to derive structural formulae for the smectite (Table 5).

Although BCD treatment has become a standard technique for removal of hydrated iron oxides from clays (Brown & Brindley 1980), the treatment alters the Fe^{2+}/Fe^{3+} ratio of clay minerals, including smectite (Rozenson & Heller-Kallai 1976, Lyle 1983, Ericsson *et al.* 1984). Moreover, Fe^{2+} in iron-rich smectite from the reducing environment of the Atlantis II Deep, equivalent to the SSA facies, has been shown by Mössbauer spectroscopy to undergo rapid (a few hours) subaerial oxidation during sampling, unless adequate precautions are taken (Badaut *et al.* 1985). Thus, in the absence of non-destructive techniques such as Mössbauer spectroscopy, and without appropriate precautions to prevent possible subaerial oxidation, it was not possible to distinguish analytically Fe^{2+} from Fe^{3+}, and total iron only is reported for the smectite compositions (Table 4). However, in the structural formulae (Table 5) proportions of di- and trivalent components have been distinguished. The latter have a systematic, yet reasoned, geochemical basis, outlined separately below for each of the three associations of smectite.

That the BCD treatment also removes iron from clay minerals, particularly iron-rich smectite (Russel *et al.* 1979), is more speculative and has not been clearly substantiated. Undoubtedly both alteration of Fe^{2+}/Fe^{3+} ratios and leaching of Fe are pH-dependent (Rozenson & Heller-Kallai 1976, Borchardt 1977), which is why the treatment is buffered to about pH 7. In addition, it is certain that alteration of the ratio is at least partly reversible (Rozenson & Heller-Kallai 1976, Ericsson *et al.* 1984). Moreover, some crystalline iron oxides, such as hematite, are resistant to the treatment (Ericsson *et al.* 1984). Even goethite can show discernible resistance to BCD reagent, as has been found in leaching experiments of my own on Red Sea sediments (unpublished). Beyond this, stable-isotope studies of clay minerals, including iron-rich smectite and use of BCD reagent, have shown the treatment to be isotopically "safe" (Cole 1985, Yeh & Savin 1976, 1977, Yeh & Epstein 1978, McMurtry & Yeh 1981). Of particular relevance to this study, previous investigations of Atlantis II Deep smectite, including composition determinations, also have used BCD treatments (Bischoff 1972, Goulart 1976, Brockamp *et al.* 1978, Singer & Stoffers 1981, Zierenberg & Shanks 1983).

It is noteworthy that the smectite analyzed by Badaut *et al.* (1985) was considered to undergo continued oxidation during more prolonged exposure to air (over a week), with the appearance of free iron oxides. However, their Mössbauer analysis of a smectite the same as that in the SSA facies was conducted on a bulk sample in its natural state. It seems more probable that the free iron oxides did not originate from smectite oxidation but from oxidation of the iron-rich amorphous phases, both abundant and extremely labile in this facies. From the foregoing observations it seems unlikely that BCD treatment removes significant Fe from smectite, and use of the reagent in this study is not only justified but necessary. Thus, the total-iron data for the smectites (Table 4) appear to be valid.

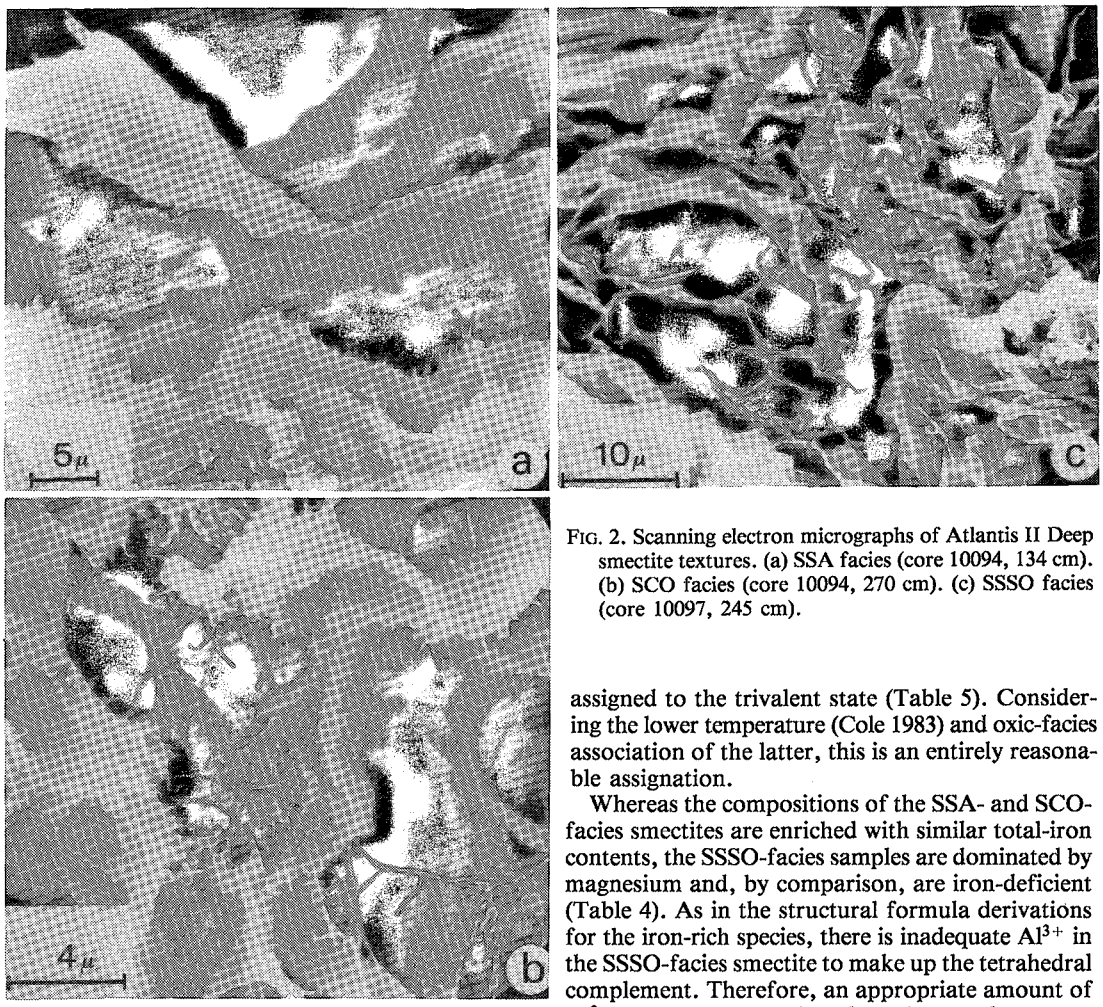

FIG. 2. Scanning electron micrographs of Atlantis II Deep smectite textures. (a) SSA facies (core 10094, 134 cm). (b) SCO facies (core 10094, 270 cm). (c) SSSO facies (core 10097, 245 cm).

From the XRD data (not illustrated) the smectites from all three facies evidently are well-crystallized. Visual characteristics of the smectites are available from a SEM examination of bulk freeze-dried sediment fragments sampled directly from the cores (Fig. 2).

SMECTITE SPECIATION

In the absence of any chemical treatment or natural alteration it has been shown that 32% of the total iron in SSA-facies smectite is Fe^{2+} in octahedral coordination (Badaut *et al.* 1985). This unique measurement has been used in calculating the structural formulae for the smectite separates from the SSA facies, where the total-iron determinations have been apportioned between Fe^{2+} and Fe^{3+} in the same ratio (Table 5). For the single smectite sample analyzed from the SCO facies, all the iron has been assigned to the trivalent state (Table 5). Considering the lower temperature (Cole 1983) and oxic-facies association of the latter, this is an entirely reasonable assignation.

Whereas the compositions of the SSA- and SCO-facies smectites are enriched with similar total-iron contents, the SSSO-facies samples are dominated by magnesium and, by comparison, are iron-deficient (Table 4). As in the structural formula derivations for the iron-rich species, there is inadequate Al^{3+} in the SSSO-facies smectite to make up the tetrahedral complement. Therefore, an appropriate amount of Fe^{3+} has been apportioned as the supplementary substituent. The greater iron fraction remaining has been assigned to octahedral coordination, entirely as Fe^{2+} (Table 5). This procedure matches the anoxic and high-temperature facies association of this smectite (Cole 1983) and duplicates the procedure used for similar material by Zierenberg & Shanks (1983).

The oxide of the SSSO facies obviously cannot be contemporaneous with the sulfide phases. Visually, the SSSO-facies sediment in core 10097 reflects considerable post-depositional disturbance (Cole 1982). It seems likely that the period of sediment disturbance was short-lived, during which time the oxide (hematite) formed diagenetically from pyrrhotite. These two minerals occur antipathetically in the SSSO facies (Cole 1982, 1983). Although the oxygen source is unknown, the oxidation period must have been short-lived if only a part of the most labile of the sulfide phases was affected. Therefore, the smectite is considered to have formed in an anoxic

environment, and the presence of hematite is irrelevant.

The structural formulae for the SSA-facies smectite are a hybrid of di- and trioctahedral character. This is confirmed in the sum of octahedral cations (Table 5) which, for ideal dioctahedral and trioctahedral structures, should be 4 and 6, respectively. By virtue of its derivation, the formula for the SCO-facies smectite displays distinct dioctahedral character, although the structure lacks divalent cations other than Fe^{2+} (Mg^{2+}, Cu^{2+}, and Zn^{2+}) by comparison to the SSA-facies smectite (Table 5). The formulae derived for the SSSO-facies smectite are distinctly trioctahedral, principally on account of its magnesium enrichment. Moreover, unlike the SSA-facies smectite, the species from the SSSO facies contains almost no Cu^{2+} or Zn^{2+} (Table 5). The absence of sulfide contamination in the SSSO separates testifies to the adequacy of the separation procedure. Thus it seems reasonable to assume that sulfide has not contaminated the SSA-facies separates, and that the trace-element enrichments are real. In addition, the separates of the SSA facies were light green, an unlikely color if they were contaminated with black sulfide material.

Distinguishing further between the two iron-rich smectites, it has been found that, whereas the anoxic variety dissolved completely during treatment with hot 50% HCl, the oxic variety suffered only partial destruction (Cole 1982). Possibly, relatively higher chemical purity in the layer of octahedra for the latter renders it more stable and with greater acid resistance.

Notwithstanding the compositional and structural differences between the three smectite species, all have similar derived composite-layer charge deficiencies (Table 5). In contrast, the smectites show non-uniform expansion behavior during glycerol solvation (Table 1) indicating diverse, and generally lower, composite-layer charges. With the exception of two samples, the layer charges are at or exceed the defined limit of 1.2 equivalents of charge per $O_{20}(OH)_4$ formula unit (Bailey 1980) which distinguishes smectite from vermiculite. By definition, smectite has a layer charge less than 1.2, whereas vermiculite has a layer charge greater. Smectite typically expands to about 18 Å spacing on exposure to glycerol, whereas vermiculite does not expand from its 14–15 Å spacings (MacEwan & Wilson 1980). The XRD data (Table 1) suggest that the species from the SSA facies is vermiculitic, and the structural formulae (Table 5) suggest that all three species are vermiculitic.

Excessively high layer charges are ubiquitous in reported structural compositions for Atlantis II Deep smectite (*e.g.*, Bischoff 1972, Zierenberg & Shanks 1983). Moreover, layer charges of deep-sea authigenic smectite often are higher than in detrital smectite formed by continental weathering (Cole & Shaw 1983a). Authigenic iron-rich smectite in Recent marine sediments frequently contains high trace-element concentrations. Cu^{2+} or Zn^{2+} substitutions for trivalent cations in the octahedral positions of dioctahedral smectite produce an increased layer charge. However, if these cations are omitted from structural-formula calculations, then even greater charges result.

The derived structural formula for the SCO-facies smectite is that of nontronite. The formulae for the SSA-facies smectite are exactly intermediate in character between the dioctahedral end-member, nontronite, and a trioctahedral iron end-member (as yet, hypothetical and unnamed). The formulae for the SSSO-facies smectite are those of saponite.

The more detailed XRD data obtained for the SSSO-facies smectite (Tables 2, 3) support the saponite speciation, although many of the results are also consistent with beidellite. Previously (Cole & Shaw 1983a, Cole 1983) the SSSO-facies smectite was described as a montmorillonite/beidellite. That conclusion was founded on the single Greene-Kelly test result (Table 3), but without the chemical and other supporting XRD analyses now available. Clearly the Mg enrichment of the SSSO facies (Cole 1982) is not accountable entirely by the presence of talc, also described previously (Cole & Shaw 1983b), nor is the smectite dioctahedral. Evidently, the Greene-Kelly test result is spurious, probably related to the anomalous layer charges in the saponite.

The saponite XRD data (Table 3) include a shoulder on the 001 reflection (air dried) for sample 247–252 cm, present with both Na^+ (9.8 Å) and Mg^{2+} (11.4 Å) as saturating cations. The shoulder is consistent with the presence of, respectively, a minor "anhydrous" component in a predominantly "monohydrate" structure (Na^+ saturating cation) and a minor "monohydrate" in a predominantly "dihydrate" structure (Mg^{2+} saturating cation) (Suquet *et al.* 1975). Complete expansion, including the shoulder, to 18 Å during glycerol and glycol treatment and with both saturating cations, rules out possible contamination by talc, or its randomly stacked variety called kerolite (unexpandable). Confirmation of this hydration interpretation is also evident from the chemical data (Table 4) where the water content of sample 247–252 cm is some 3% less than that of sample 207–212 cm. Moreover, in two XRD patterns obtained for Mg-saturated sample 247–252 cm, two higher order basal reflections are visible, corresponding to the subordinate "monohydrate". These reflections are absent from similar traces obtained for sample 207–212 cm, which occurs entirely as the "dihydrate".

Smectite Distribution

It is apparent that the previously reported oxygen

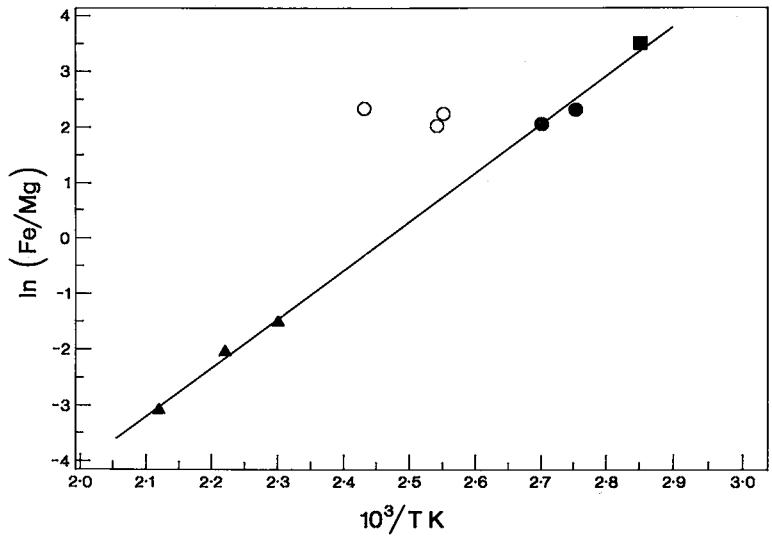

FIG. 3. Plot of ln (Fe/Mg), atomic ratios in octahedral layer (Table 5), *versus* $1/T$, reciprocal oxygen isotope temperature (Cole 1983), for smectites from cores 10094, 10096, and 10097. SSSO facies: (▲), SCO facies: (■), SSA facies, core 10094: (○), SSA facies, cores 10096 and 10097: (●).

isotope compositions (Cole 1983) and the present chemical compositions for the smectites of cores 10094, 10096, and 10097 have a qualitative coherence. The smectites appear to represent members in a chemical–mineralogical continuum of Mg/Fe fractionation, including trioctahedral/dioctahedral structural transition, as a function of spatial variations in temperature and redox conditions in the Atlantis II Deep. The highest and lowest temperature end-members are assumed to be, respectively, talc and nontronite.

A strong linear correlation of structural composition with oxygen isotope composition in Atlantis II Deep smectite has recently been demonstrated quantitatively (Zierenberg & Shanks 1988) by plotting ln (Fe/Mg), in the octahedral layer, against reciprocal formation temperature, $1/T$. Applying this same procedure, a similar strong linear correlation is evident in the smectites of this study (Fig. 3) although three samples lie distinctly to the high temperature side of the plot. The line drawn represents a best fit omitting those three, all from the SSA facies of core 10094. The latter are thought to have been influenced by a present-day temperature anomaly (Cole 1983) which may account for their behavior. The point farthest off the line represents the uppermost sample, 5–10 cm. The two remaining SSA-facies samples, each from different sites, lie on the line and presumably represent more typical behavior for this facies.

The SSA facies is equivalent to the iron-rich montmorillonite facies described by Bischoff (1969) and the SAM Zone (AM Zone outside the SW Basin) defined by Bäcker & Richter (1973). This material represents the thickest, most continuous, and uppermost facies in the Atlantis II Deep (Hackett & Bischoff 1973), and reflects depositional conditions dominant at present. The SSA-facies smectite is probably the most abundant mineral in the entire geothermal deposit, and certainly it is the iron-rich variety most commonly reported. This smectite has been variously described as a nontronite (*e.g.*, Bischoff 1972, Goulart 1976, Cole 1983, Cole & Shaw 1983a) although its partial trioctahedral character has been recognized previously (Bischoff 1972, Badaut *et al.* 1985).

Iron-rich smectite of oxic-facies association (equivalent to SCO) has been reported previously in the Atlantis II Deep (Goulart 1976), which also has been found to be trace-element depleted (Brockamp *et al.* 1978). However, neither study distinguished this smectite from the anoxic variety, as in both cases the bulk sediment contained sulfide. Thus, Brockamp *et al.* (1978) concluded that earlier reports of trace-element enrichments in Atlantis II Deep iron-rich smectite (*e.g.*, Bischoff 1972) were spurious because of sulfide contamination. Almost certainly, the sulfide in the samples of Brockamp *et al.* (1978) is extraneous, and unwittingly their data support the occurrence of a separate oxic species depleted in trace elements. However, the overall abundance and distribution of the oxic smectite remains uncertain.

Sediments recovered from the SW Basin of the

Atlantis II Deep containing anhydrite and talc veins have recently been found to include iron-bearing saponite (Zierenberg & Shanks 1983). This is equivalent to the SSSO facies which is dominated by anhydrite (Cole 1982, 1983), although the temperature range of the veins is evidently wider. Significantly, compared to veins dominated by talc, saponite associated with veins predominantly of anhydrite were found to be richer in Fe. Moreover, appropriate phase diagrams constructed for 60 and 150°C (Zierenberg & Shanks 1983) indicate that Mg saponite is favored at high temperatures, whereas cooler temperatures favor precipitation of Fe-bearing smectites.

Smectite Genesis

The origin of smectite in cores 10094, 10096, and 10097 has been discussed previously (Cole 1982, 1983, Cole & Shaw 1983a). However, from the chemical data now available two modifications are necessary.

First, it was assumed previously that kerolite in the SSSO facies fractionated all the Mg. Thus, it was asserted that the kerolite formed separately from the smectite. However, Mg enrichment in both clay minerals suggests simultaneous formation, concurrent with the sulfate and sulfide phases. The discharging brines of the present are depleted of Mg^{2+} and SO_4^{2-} (*e.g.*, Shanks & Bischoff 1977, Danielsson *et al.* 1980), but this situation has not been permanent (Bäcker & Richter 1973). Thermal events at the brine source that induce more intense activity can occur (Shanks & Bischoff 1977), resulting in enhanced Mg^{2+} and SO_4^{2-} supply. Evidently, the site of core 10097 was in close proximity to intense, though ultimately ephemeral, discharge activity. In more quiescent conditions, anhydrite and magnesium silicate precipitation are subseafloor phenomena related to basalt alteration (Pottorf & Barnes 1983). This modification precludes the requirement of an enhanced Al^{3+} supply from the incoming brine (Cole 1983).

Secondly, it was assumed previously that the two iron-rich smectites had different Fe/Si ratios, which accounted for their differences of formation temperature. However, both smectites have similar Fe/Si ratios (Table 4), so differences of Fe^{2+}/Fe^{3+} ratio must be invoked. Thus, although the contribution of Fe and Si from the respective FeO(OH) and SiO_2 precursors is constant, the proportion of oxygen contributed by each appears to have been variable. The higher temperature structures evidently incorporated a greater contribution from the isotopically lighter SiO_2, with the heavier isotope in FeO(OH) being lost during iron reduction. The oxic smectite, whose trivalent-iron content is highest and formation temperature is lowest, has therefore probably retained the greatest oxygen contribution from FeO(OH).

From the proposed formation mechanisms (Cole 1983, Cole & Shaw 1983a) there is a fundamental difference in the origins of the smectites. The Mg-rich smectite has only brine-derived SiO_2 as its oxygen source, whereas the Fe-rich smectites each has a combined source in SiO_2 and FeO(OH). However, the linear correlation of structural composition with oxygen isotope composition in the smectites (Fig. 3) regardless of this difference, suggests that isotope fractionation during clay-mineral formation is a function of temperature only, and does not include compound fractionation. Moreover, the correlation lends support both to the reliability of the chemical and isotope compositions for the smectites, and to the validity of the derivation procedure used for their structural formulae.

References

Bäcker, H. & Richter, H. (1973): Die rezente hydrothermal-sedimentäre Lagerstätte Atlantis-II-Tief im Roten Meer. *Geol. Rundschau* **62**, 697-741.

_____ & Schoell, M. (1972): New Deeps with brines and metalliferous sediments in the Red Sea. *Nature* (Phys. Sci.) **240**, 153-158.

Badaut, D., Besson, G., Decarreau, A. & Rautureau, R. (1985): Occurrence of a ferrous, trioctahedral smectite in Recent sediments of Atlantis II Deep, Red Sea. *Clay Minerals* **20**, 389-404.

Bailey, S.W. (1980): Summary of recommendations of AIPEA Nomenclature Committee. *Clay Minerals* **15**, 85-93.

Bischoff, J.L. (1969): Red Sea geothermal brine deposits: their mineralogy, chemistry and genesis. *In* Hot Brines and Recent Heavy Metal Deposits in the Red Sea (E.T. Degens & D.A. Ross, eds.). Springer-Verlag, New York.

_____ (1972): A ferroan nontronite from the Red Sea geothermal system. *Clays Clay Minerals* **20**, 217-223.

Borchardt, G.A. (1977): Montmorillonite and other smectite minerals. *In* Minerals in Soil Environments (J.B. Dixon & S.B. Weed, eds.). Soil Sci. Soc. America, Madison, Wisconsin.

Brockamp, O., Goulart, E., Harder, H. & Heydemann, A. (1978): Amorphous copper and zinc sulphides in the metalliferous sediments of the Red Sea. *Contr. Mineral. Petrology* **68**, 85-88.

Brown, G. & Brindley, G.W. (1980): X-ray diffraction procedures for clay mineral identification. *In* Crystal Structures of Clay Minerals and Their X-ray Identification (G.W. Brindley & G. Brown, eds.). Mineralogical Society, London.

Cole, T.G. (1982): *Mineralogy and Geochemistry of Metalliferous Sediments from the Bauer Deep, Southeast Pacific, and the Atlantis II Deep, Red Sea.* PhD thesis, Imperial College, London.

_____ (1983): Oxygen isotope geothermometry and origin of smectites in the Atlantis II Deep, Red Sea. *Earth Planet. Sci. Lett.* **66**, 166-176.

_____ (1985): Composition, oxygen isotope geochemistry, and origin of smectite in the metalliferous sediments of the Bauer Deep, southeast Pacific. *Geochim. Cosmochim. Acta* **49**, 221-235.

_____ & SHAW, H.F. (1983a): The nature and origin of authigenic smectites in some Recent marine sediments. *Clay Minerals* **18**, 239-252.

_____ & _____ (1983b): Kerolite associated with anhydrite in sediments from the Atlantis II Deep, Red Sea. *Clay Minerals* **18**, 325-331.

DANIELSSON, L-G., DYRSSEN, D. & GRANELI, A. (1980): Chemical investigations of Atlantis II and Discovery brines in the Red Sea. *Geochim. Cosmochim. Acta* **44**, 2051-2065.

DEGENS, E.T. & ROSS, D.A. (eds.) (1969): *Hot Brines and Recent Heavy Metal Deposits in the Red Sea.* Springer-Verlag, New York.

ERICSSON, T., LINARES, J. & LOTSE, E. (1984): A Mössbauer study of the effect of dithionite/citrate/bicarbonate treatment on a vermiculite, a smectite and a soil. *Clay Minerals* **19**, 85-91.

GOULART, E.P. (1976): Different smectite types in sediments of the Red Sea. *Geol. Jahrb.* **17**, 135-149.

HACKETT, J.P. & BISCHOFF, J.L. (1973): New data on the stratigraphy, extent, and geologic history of the Red Sea geothermal deposits. *Econ. Geol.* **68**, 553-564.

INGAMELLS, C.O. (1970): Lithium metaborate flux in silicate analysis. *Anal. Chim. Acta* **52**, 323-334.

LYLE, M. (1983): The brown-green colour transition in marine sediments: A marker of the Fe(III)-Fe(II) redox boundary. *Limnol. Oceanogr.* **28**, 1026-1033.

MACEWAN, D.M.C. & WILSON, M.J. (1980): Interlayer and intercalation complexes of clay minerals. *In* Crystal Structures of Clay Minerals and Their X-ray Identification (G.W. Brindley & G. Brown, eds.). Mineralogical Society, London.

MCMURTRY, G.M. & YEH, H-W. (1981): Hydrothermal clay mineral formation of East Pacific Rise and Bauer Basin sediments. *Chem. Geol.* **32**, 189-205.

MEHRA, O.P. & JACKSON, M.L. (1960): Iron oxide removal from soils and clays by a dithionite-citrate system buffered with sodium bicarbonate. *Proc. Nat. Conf. Clays Clay Minerals* **7**, 317-327.

POTTORF, R.J. & BARNES, H.L. (1983): Mineralogy, geochemistry, and ore genesis of hydrothermal sediments from the Atlantis II Deep, Red Sea. *Econ. Geol. Monogr.* **5**, 198-223.

ROSS, C.S. & HENDRICKS, S.B. (1945): Minerals of the montmorillonite group. *U.S. Geol. Surv. Prof. Pap.* **205B**.

ROZENSON, I. & HELLER-KALLAI, L. (1976): Reduction and oxidation of Fe^{3+} in dioctahedral smectites — 1: reduction with hydrazine and dithionite. *Clays Clay Minerals* **24**, 271-282.

RUSSELL, J.D., GOODMAN, B.A. & FRASER, A.R. (1979): Infrared and Mössbauer studies of reduced nontronites. *Clays Clay Minerals* **27**, 63-71.

SCHOELL, M. & HARTMANN, M. (1973): Detailed temperature structure of the hot brines in the Atlantis II Deep area (Red Sea). *Mar. Geol.* **14**, 1-14.

SHANKS, W.C., III & BISCHOFF, J.L. (1977): Ore transport and deposition in the Red Sea geothermal system: A geochemical model. *Geochim. Cosmochim. Acta* **41**, 1507-1519.

_____ & _____ (1980): Geochemistry, sulfur isotope composition, and accumulation rates of Red Sea geothermal deposits. *Econ. Geol.* **75**, 445-459.

SHAW, H.F. (1972): The preparation of oriented clay mineral specimens for X-ray diffraction analysis by a suction-onto-ceramic tile method. *Clay Minerals* **9**, 349-350.

SINGER, A. & STOFFERS, P. (1981): Hydrothermal vermiculite from the Atlantis II Deep, Red Sea. *Clays Clay Minerals* **29**, 454-458.

SUQUET, H., DE LA CALLE, C. & PEZERAT, H. (1975): Swelling and structural organization of saponite. *Clays Clay Minerals* **23**, 1-9.

TANNER, C.B. & JACKSON, M.L. (1947): Nomographs of sedimentation times for soil particles under gravity or centrifugal acceleration. *Proc. Soil Sci. Soc. Amer.* **12**, 60-65.

YEH, H-W. & EPSTEIN, S. (1978): Hydrogen isotope exchange between clay minerals and seawater. *Geochim. Cosmochim. Acta* **42**, 140-143.

_____ & SAVIN, S.M. (1976): The extent of oxygen isotope exchange between clay minerals and seawater. *Geochim. Cosmochim. Acta* **40**, 743-748.

_____ & _____ (1977): Mechanism of burial metamorphism of argillaceous sediments: 3. O-isotope evidence. *Bull. Geol. Soc. Amer.* **88**, 1321-1330.

ZIERENBERG, R.A. & SHANKS, W.C., III (1983): Mineralogy and geochemistry of epigenetic features in metalliferous sediment, Atlantis II Deep, Red Sea. *Econ. Geol.* **78**, 57-72.

_____ & _____ (1988): Isotopic studies of epigenetic features in metalliferous sediment, Atlantis II Deep, Red Sea. *Can. Mineral.* **26**, 737-753.

Received September 18, 1987; revised manuscript accepted April 26, 1988.